In vitro model for endogenous optical signatures of collagen

Nathaniel D. Kirkpatrick
James B. Hoying
Shaleen K. Botting
University of Arizona
Biomedical Engineering Program
Life Sciences North, Rm. 362
1501 N. Campbell Ave.
Tucson, Arizona 85724

Jeffrey A. Weiss
University of Utah
Department of Bioengineering
50 S. Central Campus Dr., Rm. 2480
Salt Lake City, Utah 84112-9202

Urs Utzinger
University of Arizona
Biomedical Engineering Program
Life Sciences North, Rm. 362
1501 N. Campbell Ave
Tucson, Arizona 85724

Abstract. Type I collagen is a major component of the extracellular matrix as well as many tissue engineered models. To understand changes in collagen related models over time, it is important to evaluate collagen dynamics with noninvasive techniques. Fluorescence spectroscopy provides a method to noninvasively measure endogenous collagen fluorescence. Additionally, second harmonic generation (SHG) imaging of collagen produces high resolution images of the fibrils. In this study, a novel *in vitro* collagen measurement chamber was developed for measurement in standard spectroscopic cuvette chambers and microscopic imaging. The fluorescence of polymerized collagen was found to be highly variable, primarily depending on incubation time after polymerization. Changes in fluorescence over time were consistent with increases at UVA excitation wavelengths ($\lambda ex = 360$ nm) and decreases at UVC excitation wavelengths ($\lambda ex = 270$ nm), suggesting changes in nonenzymatic association of the collagen fibrils. SHG imaging of the collagen suggested that a stable network formed during polymerization. Unlike the fluorescence emission, SHG images from the gels varied little with time suggesting that SHG is not as sensitive to cross-linking or fibril-fibril associated changes. The developed measurement system will allow further studies on the effect of enzymatic cleavages and structural alterations on collagen fluorescence and SHG. [DOI: 10.1117/1.2360516]

Keywords: endogenous collagen fluorescence; noninvasive monitoring of engineered tissue models; SHG imaging of collagen.

Paper 05397R received Jan. 4, 2006; revised manuscript received May 11, 2006; accepted for publication May 31, 2006; published online Oct. 24, 2006.

1 Introduction

The extracellular matrix provides a structural lattice for cells in tissue, facilitates cellular communication, and is a key component during processes such as angiogenesis and neoplasia.[1] Type I collagen, one of the main components of the interstitial matrix, exhibits both optical scattering and endogenous fluorescence, two properties that can potentially be exploited to noninvasively estimate changes in the extracellular matrix. Collagen has become an important biomarker for optical cancer diagnostic methods[2] and has been utilized as a basis for *in vitro* organotypic tissue cultures including viral models,[3] lung tissue,[4] and vascular tissue constructs.[5] We have developed a system for controlled measurements on collagen gels *in vitro* using both spectroscopic and microscopic techniques. Of particular interest in this study are collagen alterations in the context of angiogenesis in tissue engineered constructs where matrix metalloproteases (MMPs) locally modify the extracellular matrix, allowing for new blood vessel growth. It has been shown that increases in MMP-2 and MMP-9 expression occur during angiogenesis in these vascular constructs.[6] A noninvasive approach to monitor changes in collagen structure during such processes would provide further insight into extracellular matrix dynamics.

Collagen fibers are made of a triple helix of procollagen molecules based on peptide chains. Procollagen is generated by intracellular processes and then secreted for further processing by extracellular enzymes. Ultimately, individual collagen molecules assemble into bundled collagen fibrils.[7] These fibrils can be highly arranged and enzymatically cross-linked for further stability. However, in self-polymerizing collagen gels typically used in engineered constructs, this ordered assembly becomes a more random process. Thus, the corresponding optical signature of the collagen may differ from *in vivo* conditions.

Endogenous collagen fluorescence is thought to arise primarily from lysyl hydroxylase-dependent lysyl (LP) and hydroxylysyl (HP) hydroxypyridoxyline cross-links (enzymatic cross-links) between collagen fibers;[8–10] but additional fluorescence can be observed, from non-enzyme-dependent cross-linking such as glycation.[11,12] The fluorescence signature of collagen can vary with the amount of cross-linked fibrils, the organization of the collagen fibrils, and gel polymerization time. Additionally, fluorescence is dependent on environmental factors such as pH and temperature.[13,14]

Address all correspondence to Urs Utzinger, 1501 N. Campbell Ave, AHSC, Rm 8319, Tucson, AZ 85724; Tel: 520-626-9281; Fax: 520-626-2514; E-mail: utzinger@u.arizona.edu

1083-3668/2006/11(5)/054021/8/$22.00 © 2006 SPIE

Because collagen is a major contributor to endogenous tissue fluorescence and scattering, tissue phantoms based on collagen have been used to estimate the spectral contributions of the protein.[12] However, the inherent spectral variability of collagen gels has made it difficult to determine a consistent spectral signature and also one that approximates *in vivo* measurements from the extracellular matrix. It is desirable to create a standard model to assess the optical signature of collagen that can serve as a control for future perturbation measurements. The optical signature of this model should partially mimic *in vivo* extracellular signals, but its characteristics will need to be well understood with regard to polymerization, aging, and degradation.

Recently, a novel noninvasive optical technique called second harmonic generation (SHG) has shown promise for collagen measurements both *in vivo* and *in vitro*.[15–18] SHG is a nonlinear scattering process that requires a highly temporally and spatially focused laser beam. Given a noncentrosymmetric environment such as in collagen fibers, the second-order polarizability or hyperpolarizability becomes significant, resulting in second harmonic light generated at half the incident wavelength.[16] This process provides inherent, high resolution three-dimensional data when a laser is scanned through a sample because the SHG signal only arises in the focal volume of the laser beam where the incident power is high enough to achieve nonlinear effects. Consequently, SHG microscopy can potentially be used to understand collagen changes in tissue constructs at a high resolution and in a noninvasive manner. In addition, two-photon excited fluorescence (2PEF) can be obtained from collagen.[4] Simultaneous measurement of SHG and 2PEF allows for comparison between nonlinear scattered and fluorescence signals.

In this study, a novel *in vitro* collagen measurement chamber was developed for measurement in standard spectroscopic cuvette chambers as well as for microscopic imaging. Here we report the variability in the endogenous fluorescence signal based on time, polymerization, pH, and temperature. Understanding the intrinsic variability of the system will allow for accurate assessment of changes in collagen fluorescence that may result from the action of an extrinsic factor such as an enzyme. We then report results from SHG imaging of the collagen chamber with a modified laser scanning confocal microscope. High resolution imaging of collagen fibrils provides a basic understanding of collagen gel polymerization, fibril lengthening, and organization.

2 Materials and Methods

Collagen gels were reconstituted from rat tail type I collagen fragments in solution at pH=4.0 (BD Biosciences, San Jose, California). A final collagen concentration of 3 mg/ml was achieved with the addition of optically inert components consisting of 1X Hanks Balanced Salt Solution (Sigma, St. Louis, Missouri), 20-mM (4-12-hydroxyethyl)-1-(piperazine-ethanesulfonic acid) (HEPES), and purified water. A final addition of NaOH brought the solution to a pH of approximately 7.4. All of the constituents were kept on ice during the process. Following the combination of constituents, the gel solution was injected into a custom-made quartz imaging chamber (size $4.0\times1.0\times0.1$ cm) with a 1-ml syringe and kept on ice for 30 min to avoid air bubble formation during polymerization. Finally, the imaging chamber was placed in either an incubator or a temperature controlled measurement chamber at 37°C for 1 h to allow for polymerization. The collagen gel remained in the incubator between each series of measurements. Although this procedure was varied based on experimental protocol (see Sec. 3), the basic steps described above were always followed. Low pH and temperature prohibits collagen self-polymerization. A collagen gel buffered to a neutral pH but kept at low temperature allows for experimental preparation because enzymatic as well as cross-linking activity is significantly reduced.

Following polymerization, the imaging chamber was connected to a peristaltic pump for flow-through of media. Media (1X Hanks Balanced Salt Solution, 20 mM HEPES) was pumped at a rate of 100 μL/min to keep the collagen gel hydrated and to allow for introduction of system perturbations (i.e., extracellular matrix enzymes). To maintain temperature between measurements, the system was kept at 37°C in an incubator. For the addition of exogenous agents, a three-way valve was placed at the entrance port of the imaging chamber.

Fluorescence data were collected from the collagen gel constructs with a Fluorolog 3-22 in front face configuration, separating the directions of excitation and emission collection by 20 deg (JY Horiba, New Jersey). The sample was measured in a thermocontrolled cell holder. Excitation wavelengths ranged from 270 to 600 nm, while fluorescence emission was collected from 20 nm above the excitation wavelength to 20 nm below twice the excitation wavelength or 700 nm if it came first. One full measurement was collected in approximately 20 min.

Data analysis was performed primarily with MATLAB (The MathWorks, Natick, Massachusetts). Excitation emission matrices (EEMs) were assembled for initial data assessment. These EEMs were used for further spectral evaluation and statistical analysis such as principal component analysis (PCA). PCA on the spectral data pool calculates its variance structure and provides a first-order assessment of fluctuations in between our experiments. For PCA, an EEM was reorganized from a matrix to a concatenated vector of emission spectra and multiple EEMs were organized into a two-dimensional matrix, with one dimension representing the measurement and the other dimension representing the emission vectors. The covariance was calculated of the newly formed matrix followed by an eigenanalysis. The resulting eigenvectors have the length of the concatenated spectra and can be arranged back to represent an EEM. The PCA treats each fluorescence intensity as an independent value and the above described data rearrangement does not affect the eigenanalysis. Increasing the number of experiments, however, could affect the outcome of the analysis. The eigenvectors represent orthogonal basis spectra with the first eigenvector encompassing the largest amount of variance and each subsequent vector a lesser amount. Because calculating the covariance matrix includes removing the overall mean of the data, the eigenvectors describe the fluctuation around the average experiment.

Linear regression and multiple regression (JMP, SAS, Cary, North Carolina) were applied to test the significance of the decay rates and whether the rates were different from zero or different from each other.

SHG and 2PEF imaging of the collagen in the imaging chamber were performed using a Zeiss LSM 510 NLO confocal microscope coupled to a Coherent Mira 900 titanium-sapphire laser. Images were obtained using a 40×, 1.3 numerical aperture oil immersion objective (Plan-Neofluar, Carl Zeiss, Jenna, Germany). Typically, the laser was tuned to 770 nm and second harmonic light was epicollected through a custom filter (bandpass 350 to 390 nm; Chroma, Rockingham, Vermont) onto a non-descan photomultiplier tube (PMT). When measuring 2PEF and SHG simultaneously, the laser was tuned to 710 nm and SHG was reflected off a dichroic mirror (long pass 400 nm, Chroma) and collected through the aforementioned bandpass filter (350 to 390 nm) while the 2PEF was transmitted through the dichroic mirror and collected with a custom filter (bandpass 400 to 500 nm, Chroma). The laser power at the sample was always less than 40-mW average power and was adjusted along with the PMT gain to achieve strong SHG and/or 2PEF signals. For imaging, the custom quartz cover on the collagen chamber was replaced with a standard coverslip in order to optimally match the objective correction optics. Collagen gels were made in a similar manner to the process used for spectroscopy. Microscope images were processed in MATLAB for background removal. For texture features, gray-level co-occurrence matrices (GLCMs) were calculated following histogram equalization of the SHG images (MATLAB Image Processing Toolbox, The MathWorks). The features were calculated by pixel distance ranging from neighboring pixels to 80 pixels, a distance of approximately 40 μm. Texture features of particular interest included correlation, contrast, energy, and homogeneity.

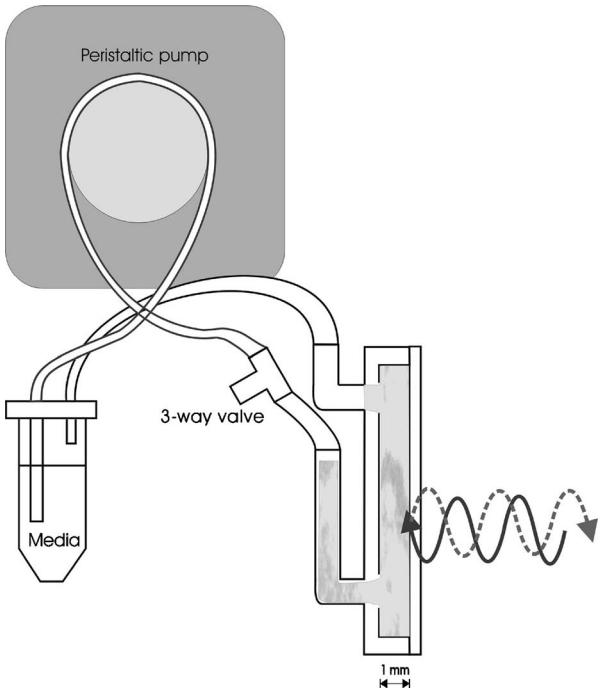

Fig. 1 Schematic of *in vitro* imaging system with quartz imaging chamber and media flow-through. Collagen gels were cast into the chamber and were measured in a fluorescence spectrometer or confocal microscope with excitation light (solid) and emitted fluorescence light (dashed). The chamber has a 1-mm optical path to allow for more specific fluorescence measurements. Media was circulated through the chamber to keep the gel hydrated and a three-way valve allowed for introduction of perturbing agents such as enzymes.

3 Results

Collagen gels were cast into a custom quartz chamber that provided minimal autofluorescence, optimal transmission in the UV, and a fixed, short optical path (1 mm). With a reduced optical path, the fluorescence properties of the collagen were measured while minimizing the scattering effects of the gel. This chamber was connected in line with a peristaltic pump for flow of media through gas permeable tubes and a three-way valve included for potential addition of outside agents (Fig. 1). In this study, multiple sets of collagen gels (five on day 1, three on day 2, and three on day 8) were measured during polymerization stages while temperature and pH experiments were completed for one collagen gel each.

3.1 *Polymerization Variation*

In order to monitor fluorescence changes during polymerization, prepared collagen in solution in the custom chamber was placed in a thermocontrolled cuvette holder of the fluorescence spectrometer maintained at 4°C. The cuvette chamber was then brought to 37°C and subsequent measurements were taken every 25 min. Average fluorescence data at a polymerization time of 175 min are depicted in the mean EEM in Fig. 2(a), with major peaks at λex=270 nm, λem=300 nm, consistent with the aromatic amino acid tyrosine[19] and at λex=360 nm, λem=450 nm, consistent with non-enzyme-dependent cross-links (e.g., vesperlysine or crossline).[11,12] An additional peak was observed at λex=320 nm, λem=400 nm (consistent with enzymatic collagen cross-links) but the fluorescence contribution from this peak was less than the peak at λex=360 nm, λem=450 nm. Differences were observed when analyzing the absolute intensity differences between the collagen at the first 37°C time point and the last time point, where increases in fluorescence associated with the λex=360 nm, λem=450 nm peak and decreases associated with the λex=270 nm, λem=300 nm were apparent (data not shown). Results from PCA on the EEMs from prepolymerization through polymerization at 175 min indicate that the majority of the variation in the gels during polymerization localizes to three areas [Fig. 2(b)]. Based on the first principal component, which represents 83% of the variation in our data, the main areas of change are consistent with the λex=360 nm, λem=450 nm peak and the λex=270 nm, λem=300 nm peak as well as variation at λex=320 nm, where a visual comparison of the first principal component with the average fluorescence emission indicates that relative spectral emission changes occur in the 320-nm excitation range.

From this analysis, differences were observed in the UVC or UVB consistent with amino acids, namely tyrosine, fluorescence (λex=270 nm) and collagen fluorescence (λex=320 to 360 nm). Because of these differences, several excitation wavelengths (λex=270, 320, 360 nm) were chosen to specifically evaluate fluorescence variations. The excitation wavelength λex=320 nm was chosen because this is the wavelength of maximal excitation of collagen cross-links HP and LP.[10] Both 270 and 360 nm were chosen because they

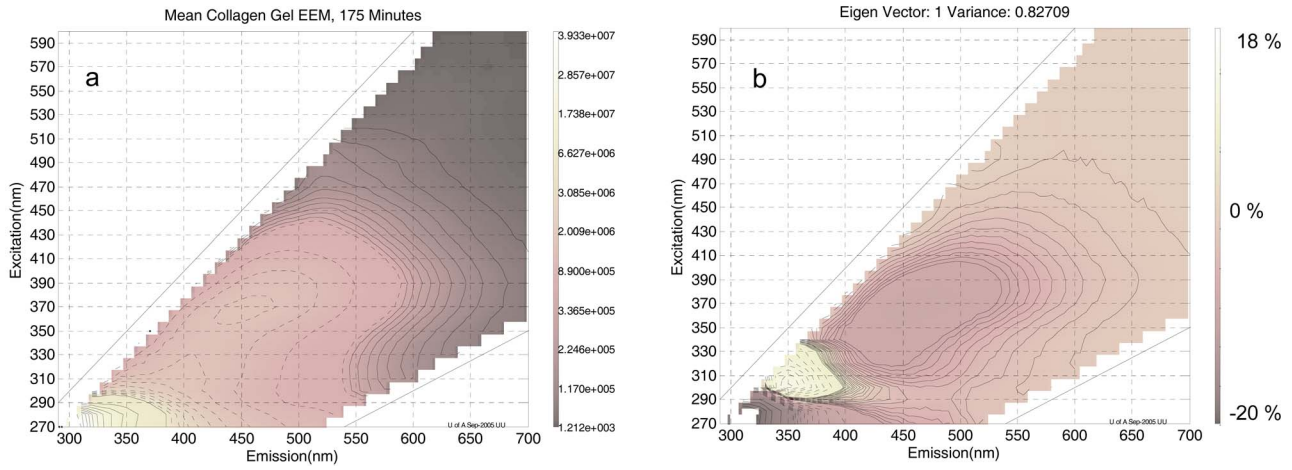

Fig. 2 (a) Average EEM from collagen gel 175 min after polymerization. Fluorescence peaks consistent with amino acids (λex=270 nm) and collagen fibrils (λex=320 to 380 nm) were observed. The scale bar represents fluorescence intensity and the contour lines are lines of equal fluorescence intensity. (b) The first eigenvector from principal component analysis suggests that most of the changes of collagen fluorescence over time (83% of the variation) correspond to three excitation bands: λex=270 to 280 nm, λex=300 to 330, λex=340 to 390 nm. The scale bar represents the relative variation.

represent a peak in our PCA of the *in vitro* collagen gel (Fig. 2).

Examining individual spectra reveals where alterations in the relative fluorescence contribution may occur. For example, in one of our experiments, we observed a significant spectral shift at λex=320 nm as the gel polymerized [Fig. 3(a)]. However, this shift was not consistently observed, providing evidence of the variability of polymerizing collagen gels and a lack of enzymatic cross-linking. Initially, a sharp fluorescence peak was located at 360 nm, but as the gel polymerized, the peak broadened and redshifted toward 400 nm, suggesting a change in the fluorescent cross-links population [Fig. 3(a)]. In the λex=360 nm spectra, the average peak fluorescence significantly increased with polymerization time [Fig. 3(b)]. The linear regression with 5 samples calculated a slope of 1.4×10^3 a.u./min with a p value of 0.012 for the hypothesis that the slope was not zero. The average peak fluorescence significantly decreased with time in the λex=270 nm spectra following polymerization [Fig. 3(c), slope $=-3.0\times10^4$ a.u./min, p=0.033, n=5]. In both Figs. 3(b) and 3(c), the point at t=−25 min corresponds to the prepolymerized gel at 4°C and pH=7, while later time points were measured at 37°C. No spectral shifts were observed in these spectra compared to the spectral changes found in the λex=320 nm spectra.

In order to express this increase in fluorescence in the 320 to 400 nm excitation range compared with the decrease in fluorescence in the 270 to 290 nm excitation range, a ratio between the 270 and 360 nm emission spectra was calculated. The ratio was determined by dividing the integrated fluorescence of the λex=270 nm spectra with the integrated fluorescence of λex=360 nm spectra. In the first day of polymerization, this ratio decreased significantly (Fig. 4, 0.027 per min, p=0.0002, n=5). As the gel aged, the ratio continued to decrease as measured on day 2 and, although the slope was slightly less than on day 1, it was not significantly different (p=0.23, n=3) than the day 1 slope (Fig. 4). By day 8, the

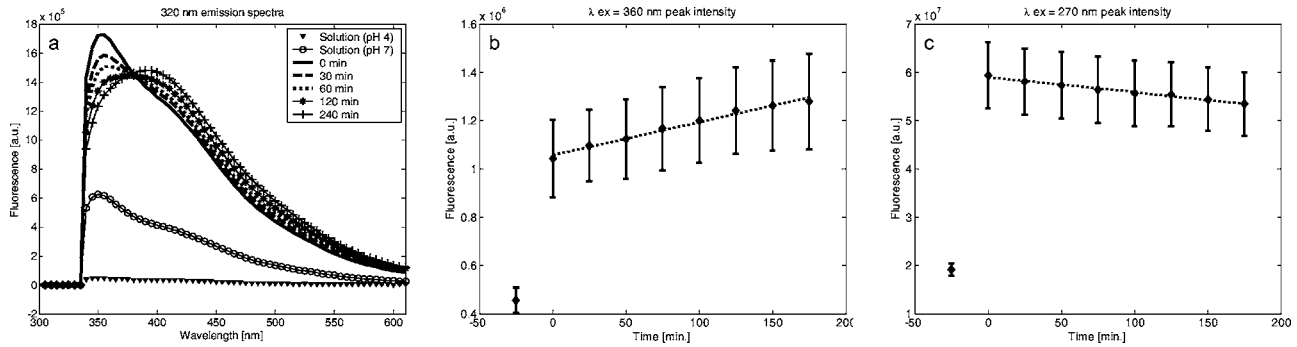

Fig. 3 (a) Emission spectra at λex=320 nm for a single collagen gel before and during polymerization. With increased polymerization time, a redshift is observed in the spectra. This dramatic shift did not occur in all samples. (b) Peak fluorescence values for emission spectra at λex=360 nm. Time point −25 min corresponds to the collagen prior to polymerization at 4°C. The dashed line signifies a linear regression line fit to the data following time point 0 min. (c) Peak fluorescence values for emission spectra at λex=270 nm. Error bars in panels (b) and (c) represent the standard deviation of the data (n=5).

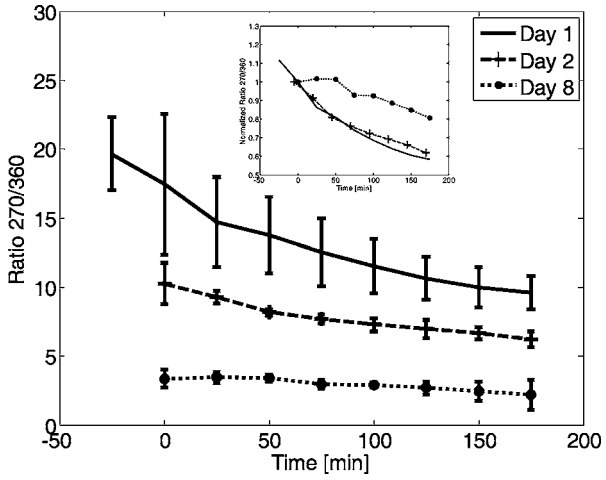

Fig. 4 Time-dependent fluorescence changes in collagen gels based on a ratio of decreasing fluorescence (λex=270 nm) to increasing fluorescence (λex=360 nm). The largest signal changes occur in the first two days with overall decrease observed out to day 8. Error bars represent the standard deviation of the data (n=5 for day 1, n=3.4 for days 2 and 8). Inset: Normalized mean ratio for comparison of slope between groups with the greatest decrease over time at day 1 and a decrease in slope or fluorescence variation by day 8.

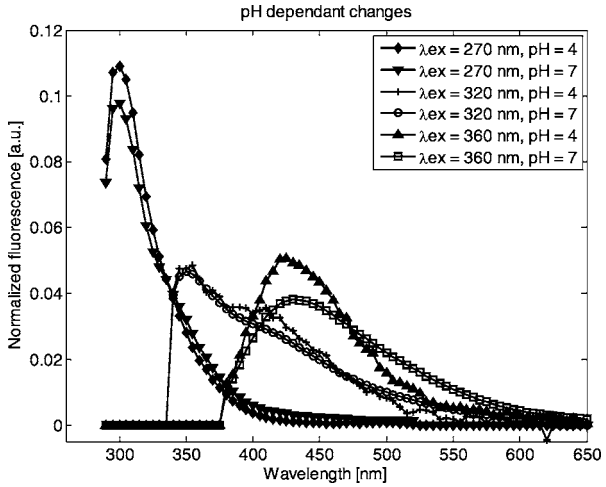

Fig. 5 Normalized fluorescence emission spectra of collagen in solution at pH=4 and pH=7.4 for λex=270 nm, λex=320 nm, and λex =360 nm. Data were normalized by the area under the curve.

change in the ratio was still apparent but the slope was significantly less (p=0.043, n=3) than on day 1 (Fig. 4). A more straightforward comparison of the slopes can be observed by normalizing the data by the intensity at 0 min, emphasizing the decreasing ratio on day 1 and day 2 while the ratio levels off by day 8 (Fig. 4, inset). The change in the ratio appears to be linked not only to gel polymerization but also the measurement itself since the value of the ratio on the last time point of day 1 is similar to that of the starting value on day 2 (Fig. 4, main figure). These data indicate significant temporal variations in fluorescence emission and intensity ratios from collagen gels from the same lot number, prepared under the same conditions.

3.2 *pH Variation*

Fluorescence spectra from the collagen in solution at a pH of 4 were compared to collagen in solution, prior to polymerization, that had been titrated to pH=7 with NaOH. As illustrated in Fig. 3(a), the spectra were significantly different in intensity, with less fluorescence emitted from the pH=4 collagen solution. For further inspection, spectra were normalized by area and the spectral shape was compared (Fig. 5). Spectral shape differed slightly for the λex=320 nm spectrum and significantly for λex=360 nm spectrum, particularly with a broader peak for the pH=7 collagen solution in the λex=360 nm spectrum. The spectra from the pH=4 collagen indicate variations due to the low fluorescence signal from this solution and subsequent decreased signal-to-noise ratio (e.g., at λex=320 nm).

3.3 *Temperature Variation*

Collagen gel fluorescence increased at all excitation wavelengths without any observable spectral shifts when the gel was cooled to 4°C (data not shown). An overall increase in fluorescence intensity of 20% was observed when comparing the EEM of the 4°C gel to the 37°C gel. When analyzing individual emission spectra, the 270 nm spectra exhibited a 13.6% increase in fluorescence when the gel was cooled down while the 320 and 360 nm emission spectra increased by 28.5 and 33.9%, respectively. An increase in fluorescence intensity is consistent with a decrease in the nonradiative pathways of energy dissipation, thereby increasing the radiative or fluorescent pathways. There were no observed spectral shifts with a decrease in temperature.

3.4 *SHG and 2PEF Imaging of Collagen Gels*

Because the collagen chamber was designed to also allow for microscopic evaluation of collagen fibril organization, SHG and 2PEF imaging of the collagen gels was performed following polymerization of the collagen. Fluorescence measured from the collagen gels was minimal at λex=780 nm (a strong SHG wavelength), a finding consistent with other reports.[15] However, when the laser wavelength was tuned to 710 nm, 2PEF from collagen could be measured along with SHG. The 2PEF signal was low and required high gain and image processing (thresholding, histogram equalization) but it overlapped with the SHG signal from the same location as shown in a two-day-old gel (Fig. 6). Appearing over a larger volume, the 2PEF signal was located around the fibril generated SHG signal. To further illustrate colocalization, areas where 2PEF intensity reached 50% of maximal range and the SHG signal reached 20% of maximal range were colored red (Fig. 6). These data suggest collagen fluorescence correlates with fibrils. SHG signatures were stronger, revealing more structural features, and required minimal image processing to achieve quality images. Further measurements for structural analysis of the collagen gels were therefore conducted with SHG imaging.

Additional SHG imaging (λex=780 nm) on two collagen gels was performed following polymerization of the collagen at day 1, day 2, and day 8 at imaging depths approximately 10 μm below the surface of the gel. For all of the SHG measurements, the structure of the gel did not vary with depth (data not shown). Multiple time point measurements were

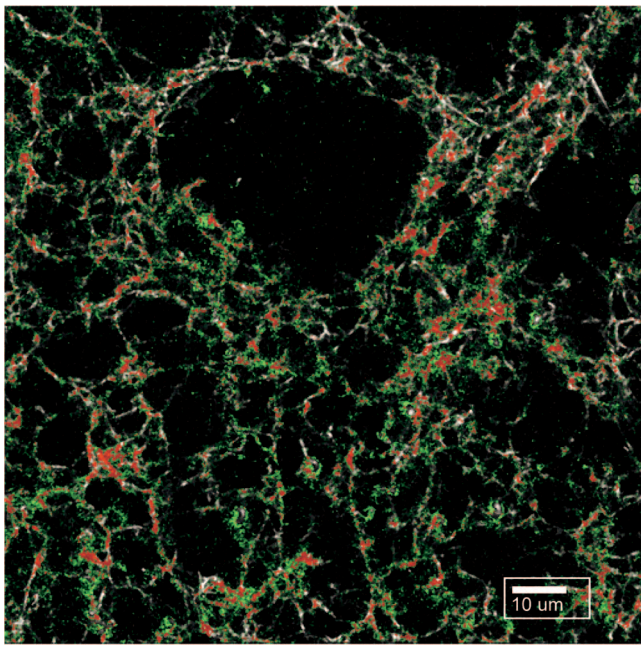

Fig. 6 2PEF (green) and SHG (grayscale) images measured from a collagen gel on day 2 (λex=710 nm). The 2PEF appears more diffuse and originating from a larger volume, while the SHG signal appears more structural. Red regions indicate strong overlap of the two signals. The scale bar represents 10 μm.

taken each day similar to the fluorescence spectroscopy measurements. On day 1 of polymerization, the fibrils in all experiments resembled a randomly oriented mesh [Fig. 7(a)]. These fibrils were short in length, suggesting minimal fibril elongation during polymerization. Based on the correlation of the image intensity levels, which were calculated over a distance of up to 80 pixels (~40 μm), the collagen structure did not change substantially over two-and-a-half hours [Fig. 7(a), data from all day 1 measurements]. Other texture features such as the intensity, homogeneity, and contrast of the images also indicated little change in the texture of the images (data not shown). At day 2, SHG images were similar to images at day 1 (data not shown) as was the correlation of the image intensity levels [Fig. 7(b), n=8 for each day]. When measured at day 8, no changes were visually perceived in the SHG images while the correlation data at day 8 seemed to reach lower levels at larger pixel distances compared to days 1 and 2 [Fig. 7(b)]. However, the differences did not exceed the standard deviation of the data.

4 Discussion

Although the spectral changes observed in Fig. 3(a) did not occur in all measurements, the figure illustrates an interesting phenomenon that may explain the cross-linking behavior in this system. Collagen cross-link fluorescence typically exhibits a peak between 380 and 400 nm when excited at 320 nm.[10] This is consistent with fluorescence from LP and HP cross-links, spectra that appear to be consistent with the prepolymerized gel illustrated in Fig. 3(a). The broader and shifted fluorescence observed after self-assembly may be due to non-enzyme-dependent cross-links. This process is commonly associated with glycation between fibers but may occur through other nonglycation processes in this *in vitro* system as glucose was not available as a substrate. Furthermore, the lack of a λex=320 nm, λem=400 nm enzymatic cross-linking peak compared to the dominant λex=360 nm, λem=450 nm non-enzyme-dependent cross-linking peak lends support for this model to be used to study enzymatic cross-linking events because the background contribution from these cross-links is minimal.

Most importantly for this study, an understanding of the dynamics of collagen gel fluorescence was ascertained. Because alterations in collagen fluorescence due to extrinsic factors are integral to noninvasively monitoring collagen gel transformations *in situ* (for example, to study organotypic tissue cultures or vessel growth), it is key to model intrinsic collagen changes and incorporate this fluorescence as a signal contributor. Changes in the fluorescence between unpolymerized and polymerized collagen suggest that modeling the collagen fluorescence signature based on liquid solutions may not be representative of physiologically relevant conditions. Data from this study also indicate that polymerization during the first day results in a highly variable fluorescence signal, consistent with alterations in cross-link fluorescence and decreases in fluorescence consistent with amino acids. As the gel aged, fluorescence variations decreased but the same trend still occurred even after eight days of incubation. Our data indicate that the rate of change may be predictable and mathematical background removal could be applied. The removal of the background variation is most appropriate when the variation is smallest as observed on day 8, suggesting that fluorescence studies in collagen-based *in vitro* cultures would be best measured at later time points.

Besides the fluorescence variations due to polymerization effects, fluorescence variations due to temperature and pH were also observed. A decrease in temperature in the polymerized collagen resulted in increased fluorescence intensity without spectral shifts; however, shorter excitation wavelengths were less affected. On the other hand, an increase in the pH of the unpolymerized collagen resulted in both changes in spectral shape and substantial increase of fluorescence intensity. Careful consideration is necessary when developing a collagen model to account for these extraneous factors supporting the need for a controlled environment such as the system developed in the study for measuring engineered tissue or tissue phantoms with optical methods.

Because fluorescence spectroscopy provides an overall measure of collagen signals, it is also useful to examine the collagen microstructure at the fibril level. 2PEF can be used as a three-dimensional microscopic imaging technique; however, the contrast obtained with SHG microscopy is greater, and it is better suited to study the structure of collagen fibrils. With its inherent optical sectioning capability, SHG imaging provides a high resolution three-dimensional view of collagen fibril formation. Using our custom designed collagen chamber, collagen fibril organization was imaged following collagen gel polymerization. The 2PEF signal from the collagen gel was low, diffuse, and originated from larger volumes than the SHG signal but it confirmed fluorescence arose from similar regions to the stronger SHG signal. Regions where the 2PEF strongly overlaps with the SHG may indicate areas of

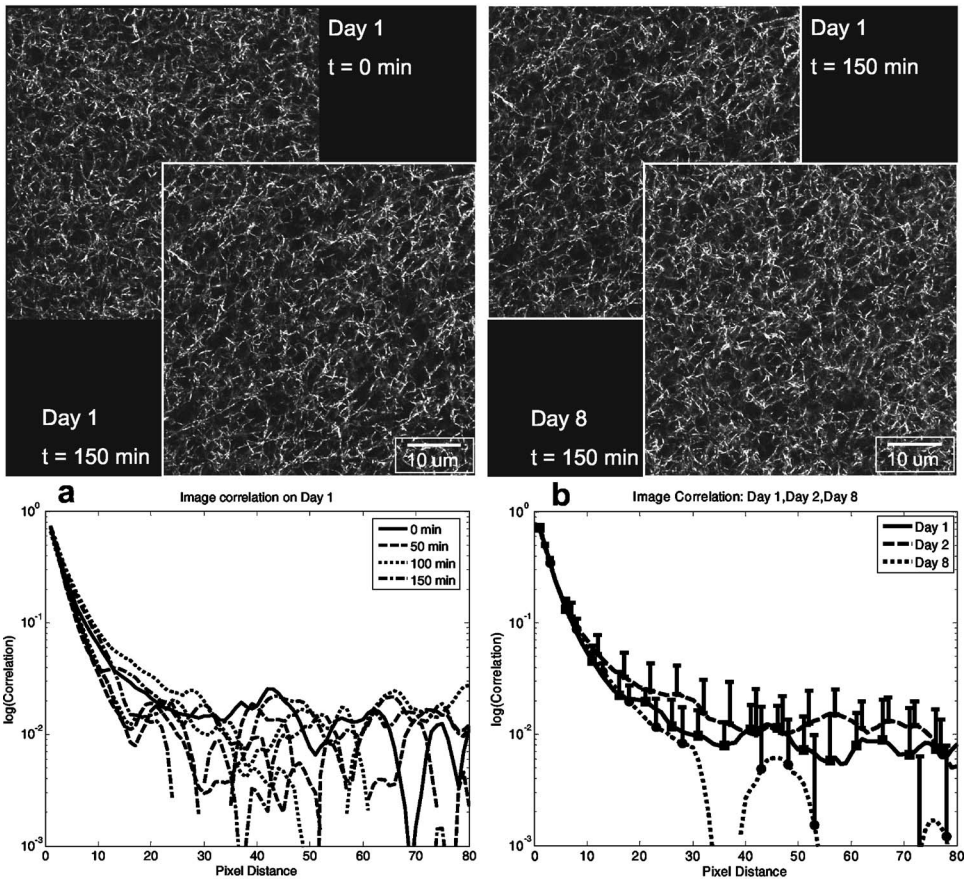

Fig. 7 (a) SHG images (λex=780 nm) measured from a collagen gel in the *in vitro* chamber on day 1, soon after polymerization (t=0 min) and at a similar location at t=150 min along with the logarithm of the correlation of pixel intensity as function of neighboring pixel distance (80 pixels ~40 μm). Fibrils appear short in length and randomly oriented. The scale bar represents 10 μm. Gray-level correlation is presented for two gels at four time points and no trend is observed over a time scale of 150 min. (b) SHG images from day 1 and day 8 appear structurally similar. The logarithmic plot of the pixel correlation indicates that the average correlation on day 2 is similar to day 1 but appears to be less on day 8 at larger pixel distances. However, differences do not exceed one standard deviation. The scale bar represents 10 μm and the error bars indicate standard deviation of eight measurements.

bundling or spontaneous cross-linking in the fibrils. Our SHG data suggest the collagen fibrils do not elongate, but seem to maintain a densely packed mesh over time. Unlike the fluorescence spectroscopy data, the SHG images from the gels varied little with time. These data suggest that SHG, being highly dependent on structure, is not as sensitive to cross-linking or fibril-fibril associated changes. Taken together, the SHG measurements provided high resolution data from collagen fibrils while the fluorescence spectroscopy measurements were sensitive to nonenzymatic association of the collagen fibrils. SHG data from collagen may be most useful for applications interrogating structural information such as invasion of cells into the extracellular matrix while fluorescence data supports questions focused on cross-linking events such as changes in collagen due to glucose-related cross-linking in diabetics.

5 Conclusion

Variations and origins of *in vitro* collagen fluorescence were assessed with a custom-made culture and measurement system. Collagen fluorescence increased with polymerization and remained highly variable during measurements. This fluorescence is consistent with an increase in cross-links that are most likely nonenzymatic in nature. SHG imaging of the collagen gel suggested that the collagen assembled into a short-fibril mesh that remained stable with time. The model presented here shows promise to further correlate optical signatures with enzymatic cleavages, enzymatic and nonenzymatic cross-linking, and microstructural changes based on fluorescence spectroscopy and SHG imaging.

Acknowledgments

This work was supported by the U.S. National Institutes of Health Grants No. HL077683 and CA098341 and by training fellowships from the BIO5 Institute of the University of Arizona and ARCS Foundation Arizona Chapter.

References

1. K. Wolf and P. Friedl, "Functional imaging of pericellular proteolysis in cancer cell invasion," *Biochimie* **87**(3–4), 315–320 (2005).
2. I. Georgakoudi, B. C. Jacobson, M. G. Muller, E. E. Sheets, K. Badizadegan, D. L. Carr-Locke, C. P. Crum, C. W. Boone, R. R. Dasari, J. Van Dam, and M. S. Feld, "NAD(P)H and collagen as *in vivo* quantitative fluorescent biomarkers of epithelial precancerous changes," *Cancer Res.* **62**(3), 682–687 (2002).

3. C. Meyers, "Organotypic (raft) epithelial tissue culture system for differentiation-dependent replication of papillomavirus," *Methods Cell Sci.* **18**(3), 201–210 (1996).
4. A. Agarwal, M. L. Coleno, V. P. Wallace, W. Y. Wu, C. H. Sun, B. J. Tromberg, and S. C. George, "Two-photon laser scanning microscopy of epithelial cell-modulated collagen density in engineered human lung tissue," *Tissue Eng.* **7**(2), 191–202 (2001).
5. B. R. Shepherd, H. Y. Chen, C. M. Smith, G. Gruionu, S. K. Williams, and J. B. Hoying, "Rapid perfusion and network remodeling in a microvascular construct after implantation," *Arterioscler., Thromb., Vasc. Biol.* **24**(5), 898–904 (2004).
6. L. Krishnan, J. B. Hoying, H. Nguyen, H. Song, and J. A. Weiss, "Angiogenesis and the extracellular matrix: Changes in construct mechanics, gene expression, and protease activity during angiogenesis," *Proc. Natl. Acad. Sci. U.S.A.* (in preparation).
7. H. Lodish, *Molecular Cell Biology*, W. H. Freeman, New York (1999).
8. R. A. Bank, S. P. Robins, C. Wijmenga, L. J. Breslau-Siderius, A. F. Bardoel, H. A. van der Sluijs, H. E. Pruijs, and J. M. TeKoppele, "Defective collagen crosslinking in bone, but not in ligament or cartilage, in Bruck syndrome: Indications for a bone-specific telopeptide lysyl hydroxylase on chromosome 17," *Proc. Natl. Acad. Sci. U.S.A.* **96**(3), 1054–1058 (1999).
9. D. R. Eyre, T. J. Koob, and K. P. Van Ness, "Quantitation of hydroxypyridinium crosslinks in collagen by high-performance liquid chromatography," *Anal. Biochem.* **137**(2), 380–388 (1984).
10. J. R. Veraart, S. J. Kok, J. M. TeKoppele, C. Gooijer, H. Lingeman, N. H. Velthorst, and U. A. Brinkman, "Capillary electrophoresis of the collagen crosslinks HP and LP utilizing absorbance, wavelength-resolved laser-induced fluorescence and conventional fluorescence detection," *Biomed. Chromatogr.* **12**(4), 226–231 (1998).
11. R. A. Bank, B. Beekman, N. Verzijl, J. A. de Roos, A. N. Sakkee, and J. M. TeKoppele, "Sensitive fluorimetric quantitation of pyridinium and pentosidine crosslinks in biological samples in a single high-performance liquid chromatographic run," *J. Chromatogr., B: Biomed. Sci. Appl.* **703**(1–2), 37–44 (1997).
12. K. Sokolov, J. Galvan, A. Myakov, A. Lacy, R. Lotan, and R. Richards-Kortum, "Realistic three-dimensional epithelial tissue phantoms for biomedical optics," *J. Biomed. Opt.* **7**(1), 148–156 (2002).
13. J. R. Lakowicz, *Principles of Fluorescence Spectroscopy*, Kluwer Academic/Plenum, New York (1999).
14. W. Zhong, P. Urayama, and M. A. Mycek, "Imaging fluorescence lifetime modulation of a ruthenium-based dye in living cells: the potential for oxygen sensing," *J. Phys. D* **36**, 1689–1695 (2003).
15. W. R. Zipfel, R. M. Williams, R. Christie, A. Y. Nikitin, B. T. Hyman, and W. W. Webb, "Live tissue intrinsic emission microscopy using multiphoton-excited native fluorescence and second harmonic generation," *Proc. Natl. Acad. Sci. U.S.A.* **100**(12), 7075–7080 (2003).
16. R. M. Williams, W. R. Zipfel, and W. W. Webb, "Interpreting second-harmonic generation images of collagen I fibrils," *Biophys. J.* **88**(2), 1377–1386 (2005).
17. E. Brown, T. McKee, E. di Tomaso, A. Pluen, B. Seed, Y. Boucher, and R. K. Jain, "Dynamic imaging of collagen and its modulation in tumors *in vivo* using second-harmonic generation," *Nat. Med.* **9**(6), 796–800 (2003).
18. A. Zoumi, A. Yeh, and B. J. Tromberg, "Imaging cells and extracellular matrix *in vivo* by using second-harmonic generation and two-photon excited fluorescence," *Proc. Natl. Acad. Sci. U.S.A.* **99**(17), 11014–11019 (2002).
19. T. Vo-Dinh, *Biomedical Photonics Handbook*, CRC Press, Boca Raton, FL (2003).